Available online at www.sciencedirect.com
SCIENCE DIRECT
ELSEVIER
Earth and Planetary Science Letters 237 (2005) 370–386
EPSL
www.elsevier.com/locate/epsl

An evaluation of quantitative reconstruction of past precipitation records using coral skeletal Sr/Ca and $\delta^{18}O$ data

Chuan-Chou Shen [a,*], Typhoon Lee [b], Kon-Kee Liu [c], Huang-Hsiung Hsu [d], R. Lawrence Edwards [e], Chung-Ho Wang [b], Meng-Yang Lee [f], Yue-Gau Chen [a], Hung-Jen Lee [g], Hsiao-Tien Sun [a]

[a] *Department of Geosciences, National Taiwan University, Taipei 106, Taiwan, ROC*
[b] *Institute of Earth Sciences, Academia Sinica, P.O. Box 1-55, Nankang, Taipei 115, Taiwan, ROC*
[c] *Institute of Hydrological Sciences, National Central University, Jhongli 320, Taiwan, ROC*
[d] *Department of Atmospheric Sciences, National Taiwan University, Taipei 106, Taiwan, ROC*
[e] *Department of Geology and Geophysics, University of Minnesota, Minneapolis, MN 55455, USA*
[f] *Department of Science Education, Taipei Municipal Teachers College, Taipei 100, Taiwan, ROC*
[g] *National Museum of Marine Biology and Aquarium, Pingtung 944, Taiwan, ROC*

Received 8 June 2004; received in revised form 28 April 2005; accepted 24 June 2005
Available online 8 August 2005
Editor: E. Boyle

Abstract

Coupled records of $\delta^{18}O$ and Sr/Ca in *Porites* coral have been used to derive hydrological conditions by removing the Sr/Ca-inferred temperature component from the $\delta^{18}O$ signal. Nanwan, a semi-enclosed bay in southern Taiwan, provides an opportunity to demonstrate the feasibility of quantitatively reconstructing past precipitation history. Recurrence of seawater $\delta^{18}O$ offsets between wet and dry seasons in the early 1990s is well correlated with the precipitation record. Even though the hydrological signal only accounts for 20% of the total annual coral $\delta^{18}O$ variation of ca. 1‰, offsets can be found in the residual $\delta^{18}O$ of modern corals after removing the thermal effect, which contributes to the other 80%. The observed timing and amplitude of the seasonal seawater $\delta^{18}O$ offsets in Nanwan and their correlation with precipitation are reproduced by hydrological models. In the mid-Holocene, the seasonal anomaly of residual $\delta^{18}O$ was twice that of the modern value based on the 9-yr Sr/Ca–$\delta^{18}O$ data recorded in a 6.73-ka *Porites* coral. Hydrological models suggest an annual rainfall of 1800–3000 mm/yr at the window during mid-Holocene, 20% higher than that of the average of 30-yr modern instrumental records of 1500–2500 mm, consistent with the qualitative pollen record from lake sediments. The seasonal decrease of residual $\delta^{18}O$ in 5 of 9 yr was earlier than the increase of the coral Sr/Ca-inferred temperature, which implies that these rainy seasons probably occurred from the early–mid-spring to mid-summer, earlier than that from late spring to late summer today. The driving force may be related to the changes of solar insolation and the East Asian monsoon. It is cautioned that the variability of hydrographic conditions imposes restrictions on a precise calculation of the

* Corresponding author. Tel.: +886 2 3366 5878; fax: +886 2 3365 1917.
E-mail addresses: river@ntu.edu.tw (C.-C. Shen), typhoon@gate.sinica.edu.tw (T. Lee), kkliu@cc.ncu.edu.tw (K.-K. Liu), hsu@atmosl.as.ntu.edu.tw (H.-H. Hsu), edwar001@tc.umn.edu (R.L. Edwards), chwang@earth.sinica.edu.tw (C.-H. Wang), monyoung@mail1.tmtc.edu.tw (M.-Y. Lee), ygchen@ntu.edu.tw (Y.-G. Chen), lec@nmmba.gov.tw (H.-J. Lee).

0012-821X/$ - see front matter
doi:10.1016/j.epsl.2005.06.042

amount of paleo-precipitation. The dynamic nature of local tectonics, monsoons and water circulation should be further addressed to precisely quantify precipitation over the past 10,000 yr from coral geochemical records.

Keywords: precipitation; coral; Sr/Ca; $\delta^{18}O$; Holocene; climate

1. Introduction

Precipitation is one of the most important climatic variables. Compared with temperature, rainfall is much more variable, often changing by more than 100% of the mean value from year to year. The fluctuation of precipitation that may cause either water shortage or flooding is a particularly serious problem for the east and south Asia, where half of the world's population resides [1]. In this region, the temporal and spatial distribution of rainfall and its overall amount are dominated by monsoons, thus highly seasonal and showing large and so far unpredictable annual variations. Failures of monsoonal rain has led to many disastrous political and economic upheavals in history. Quantitative reconstruction of past precipitation records from proxies may extend the existing records considerably and facilitate statistics for better understanding of natural cycles and, therefore, should be a scientific endeavor of first-order importance.

Paleo-precipitation is difficult to quantify precisely. There are few proxies for rainfall that are quantitative, reliable, and with better than seasonal time resolution. Oxygen isotopic composition of marine carbonate depends on both its crystallization temperature and the oxygen isotopic composition of the ambient seawater [2,3], which can be affected by rainfall. Coral $\delta^{18}O$ is of particular interest because of its annual growth bands and high time resolution (better than monthly). However, if one wishes to recover the rainfall effect, the thermal effect must either be negligibly small or correctable. Examples of the former are sites near the equator where the seasonal sea surface temperature (SST) variation is intrinsically small; thus over 100-yr-long records of large rainfall variations controlled by El Niño-Southern Oscillation (ENSO) or monsoons have been retrieved directly from coral $\delta^{18}O$ variations [4–13]. In general the thermal effects must first be corrected using SST estimated by other independent means in order to use coral $\delta^{18}O$ as a proxy for rainfall.

High precision Sr/Ca ratio in coral *Porites* may serve as a high-resolution proxy for SST [14–20]. The oxygen isotopic variation coupled with precise determination of Sr/Ca ratio offers an excellent opportunity for determining both rainfall and SST from the same coral samples. The method is based on the fact that coral Sr/Ca is controlled by SST and seawater Sr/Ca, and $\delta^{18}O$ is influenced by SST and seasonal variation of seawater $\delta^{18}O$ ($\delta^{18}O_{sw}$) caused by local rainfall and salinity change. The residual $\delta^{18}O$, which is denoted as $\Delta\delta^{18}O$, is determined by removing the isotopic shift associated with the temperature anomaly estimated from Sr/Ca in the same coral samples. It may, therefore, reflect the variation of $\delta^{18}O_{sw}$ and the salinity anomaly. An early attempt by McCulloch et al. [15] subtracted the SST effects on coral $\delta^{18}O$ using SST estimated from coral Sr/Ca. The residual variation in coral $\delta^{18}O$ for the Greater Barrier Reef of Australia was shown to correlate with the freshwater runoff from a nearby major river. This enabled the reconstruction of past flood events related to ENSO cycles in the western tropical Pacific corals. Coupled measurements of coral skeletal Sr/Ca and $\delta^{18}O$ have subsequently been applied to near-term and Holocene climatic and environmental changes [18–25].

The application of the coupled coral Sr/Ca–$\delta^{18}O$ technique to reconstruct high-resolution seasonal precipitation in the past is still a challenge constrained by the following factors. (1) In most previous studies, the $\delta^{18}O_{sw}$ component contributed a significant portion to annual coral $\delta^{18}O$ range. Except the equatorial zone and settings with tremendous freshwater input, the hydrological component is generally less than the thermal component in the tropics and subtropics. For example, changes in $\delta^{18}O_{sw}$ account for 39% of the total $\delta^{18}O$ coral signal at Rarotonga located at 21.5°S [22]. The correlation between small hydrological signals in coralline skeleton and precipitation record should be further clarified. (2) The amplitude of seasonal $\delta^{18}O_{sw}$ variation was often assumed insignificant when establishing $\delta^{18}O$–SST relationship [26]. If the seasonal

variation is too strong, it may throw the calibration off. Only at a few sites, actual records of in situ SST, salinity and precipitation have been used for calibration [23,27]. Alternatively, Gagan et al. [18,28] established coral *Porites* δ^{18}O–SST relationship during drought years. (3) Coral chemical and isotopic compositions are affected by vital effects, including metabolic factor by the micro-environments created by its symbiotic algae and kinetic behavior of skeletal growth, microchemical heterogeneities and environmental conditions [26,29–39]. Biases derived from these factors should be insignificant.

Accordingly, a careful and quantitative consideration of this coral Sr/Ca–δ^{18}O approach in a well-characterized locale with well-known hydrography is needed to gain more insight in order to fully realize the promise of this tool. Contemporary seasonal $\delta^{18}O_{sw}$ change should be well monitored and modeled quantitatively in terms of its contributing water components such as rainfall and different seawater masses. Moreover, various hydrological signals should also be reliably marked in the modern corals. The purpose of this paper is to report the results of such an evaluation conducted at a long-term monitored site inside a national park in southern Taiwan, where our previous calibration of the *Porites* coral Sr/Ca–SST relationship was determined [16]. This paper describes monthly measurements of seawater Sr/Ca, δ^{18}O, and salinity in a semi-enclosed embayment near the water intake of a nuclear power plant in the early 1990s. We present a continuous record of calculated modern $\delta^{18}O_{sw}$ derived from Sr/Ca and δ^{18}O data in a living *Porites* coral head and establish its relationship with precipitation. We then demonstrate the relationship between annual rainfall and in situ measured- and coral-based δ^{18}O offsets between wet and dry seasons using a mixing model with endmembers representing the freshwater input and two seawater masses. Finally, we apply this relationship to reconstruct paleo-rainfall records using a 6.73-ka fossil coral in the same bay aiming for future improvements of this type of study.

2. Site, samples, and measurements

Nanwan (121°E, 22°N), a part of the Kenting National Park, is a semi-enclosed basin on the southern tip of Taiwan with a seamount to the south (Fig. 1). It

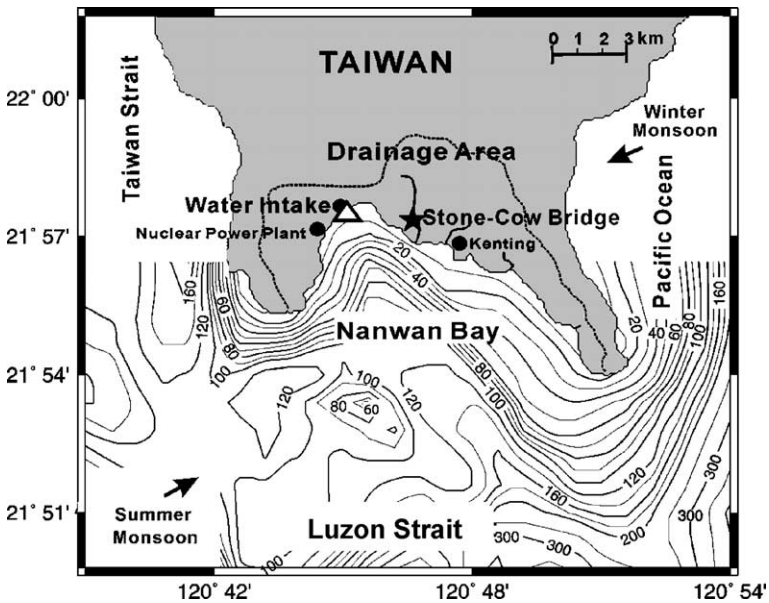

Fig. 1. Map of Nanwan Bay in Kenting National Park, southern Taiwan. Living coral head *P. lutea* (triangle symbol) and seawater samples were collected at the water intake channel of the Third Nuclear Power Plant. A 6.73-ka fossil *Porites* coral (star) was obtained near Stone-Cow Bridge. In summers the southwestern monsoon prevails from the South China Sea and precipitation occurs, and in winters southern Taiwan is located around the margin of the cold northeastern monsoon from Siberia.

opens southwards to face the Luzon Channel which is the only deep channel connecting the South China Sea to the Philippine Sea. Its hydrography has received considerable attention over two decades [40–43]. The surface seawater from the Luzon Channel flows into the bay over the seamount, ~ 50 m below sea surface. No major river empties into Nanwan, but cold upwelled seawater enters the bay daily [41–43]. The local climate is typical of that for the subtropics in the East Asian monsoon area. The onset of the southwest monsoon over the South China Sea in May begins to bring rain. This is augmented in July to September by rainfall from typhoons, which usually originate over the western North Pacific and approach from the southeast. More than 90% of the yearly precipitation, which averages 2000 ± 500 mm (1σ, 1971–2000 A.D.), falls in the wet season from May to early October. This distinct wet–dry seasonal pattern for rainfall is obvious from the monthly precipitation for 1992–1995 plotted in Fig. 2. The periodic salinity variation, from ~ 33.5‰ in wet seasons to ~ 34.4‰ in dry seasons, was revealed by a long-term program of monitoring the influence of the nuclear power plant in Nanwan from 1979 to 1991 [40]. With the sampling method described by Shen et al. [16], we collected seawater samples from the water intake channel of the nuclear power plant located at the northwestern corner of Nanwan once a month throughout 1993 and then sporadically in 1994 and 1995.

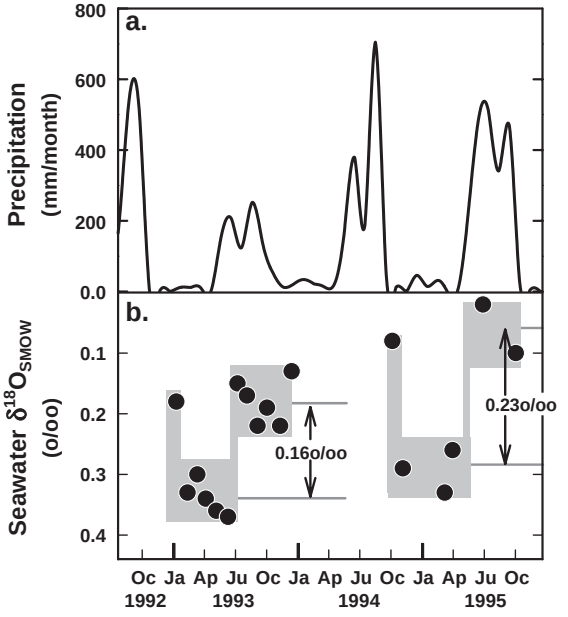

Fig. 2. Four-year, 1992–1995, (a) monthly precipitation data at Kenting area and (b) the variation of measured $\delta^{18}O_{sw}$ in Nanwan from 1993 to 1995. Rainfall increases from May to September (solid line), but there is little rainfall during other months. The seasonal variations of $\delta^{18}O_{sw}$ (gray region with solid circles) depend on the annual precipitation.

With mean SST between 22 and 28 °C, Nanwan is ideal for *Porites* coral growth. One living coral head of *P. lutea* with a growth rate of 20 mm/yr was collected at the water intake channel in 1993. One 300-mm-long fossil *Porites* coral sample was obtained from a 4-m fossil coral colony 28 m above the present sea level, at a site 1 km to the west of the Stone-Cow Bridge (Fig. 1). U and Th were separated with chemical purification methods [44]. Its ^{230}Th age is 6730 ± 32 BP (2σ) determined by inductive coupled plasma mass spectrometry (ICPMS) techniques [45]. The corrected ^{14}C age is 6582–6783 cal BP [46]. The corresponding uplift rate of 3.5 mm/yr is consistent with those between 3 and 6 mm/yr at the Stone-Cow Bridge area [47,48]. The growth rate was 15 mm/yr. A 127-mm (9-yr)-long sample was selected for tracer and isotope analyses. The sample was well preserved and X-ray diffraction showed only aragonite [49]. The intra-skeletal fine structure, the uranium concentration (2.8 ppm), the initial δ^{234}U value (146.6 ± 1.8‰, 2σ) and the consistency between ^{230}Th and ^{14}C ages all suggest the fossil sample is pristine.

A method of sample treatment was devised by modifying a procedure in the previous study by Shen et al. [16]. Corals were sectioned into 5–10 mm thick slices, immersed in 10% sodium hyperchlorite for at least 1 d, washed with deionized water, and dried at 50 °C in an oven. Cubes, ~ 12 per year, were cut along the axis of the maximum growth rate with a micro-surgical subsampling technique [50]. In an ultrasonic bath, the cubes were treated with sodium hyperchlorite, D.I. water, and then with 10^{-3} N nitric acid to dissolve the carbonate dust from cutting during subsampling. For modern corals, cubes were crushed and homogenized. Most of the samples were used for oxygen isotopic analysis and a small aliquot (50 μg) for Sr/Ca determination. For fossil samples, two parallel monthly resolution

cubes (1–2 mm^3) were cut at the same horizon and went through the cleaning process together. One cube was used for oxygen isotopic analysis and the other one for Sr/Ca ratio determination.

Oxygen isotopic analyses were performed on a SIRA-10 or a MAT-252 in the Institute of Earth Sciences, Academia Sinica for seawater and modern corals, and on a MAT-DELTA in the Department of Geosciences, National Taiwan University for the 6.73-ka coral, with an external error of 0.06‰ (1σ). An automated system for isotopic equilibration of CO_2 and H_2O by Brenninkmeijer and Morrison [51] was used for water $\delta^{18}O$ analysis. Isotopic composition calibration on 3 different mass spectrometers was accomplished with five laboratory standards, including MBS, MAS, HPM230, Merck and Hanawa, that were corrected regularly with two international carbonate standards, NBS-19 and NBS-18. Sr/Ca concentration ratios were determined on a thermal ionization mass spectrometer, MAT-262, with a reproducibility of ± 0.44‰ (2σ) using ^{42}Ca–^{44}Ca–^{84}Sr triple spike isotope dilution techniques [16,52]. The coral and seawater $\delta^{18}O$ values (‰) are expressed relative to the VPDB and VSMOW reference standards, respectively. The error given in this paper is one standard deviation unless otherwise noted.

3. Results and discussion

3.1. Directly measured seawater $\delta^{18}O$

The variation of coastal $\delta^{18}O_{sw}$ predominantly reflects the influx of ^{18}O-depleted freshwater, either as direct rainfall or as runoff from the watersheds of rivers. In Fig. 2 we show the directly measured $\delta^{18}O_{sw}$ in Nanwan from 1993 to 1995, plotted in comparison with the monthly rainfall of the region. In dry seasons, $\delta^{18}O_{sw}$ hovered around 0.32‰. In wet seasons, seawater in Nanwan showed offsets in $\delta^{18}O$ toward lighter oxygen because of rain. The seasonal $\delta^{18}O_{sw}$ offsets (differences of $\delta^{18}O_{sw}$ values between wet and dry seasons) are only several times the σ value so that we characterize them with step functions to illustrate the differences between the mean $\delta^{18}O$ values for the dry and wet seasons. The $\delta^{18}O_{sw}$ offset was 0.16 ± 0.05‰ in 1993, a drought year with only 994 mm precipitation. It became 0.23 ± 0.05‰ in 1995, a more typical year with 2099 mm rain. Despite the fact that offsets are only 2.5–4 times the analytical error, they are still significant and correlate with annual precipitation.

Nanwan $\delta^{18}O_{sw}$ did not shift until 1–1.5 months after the change between the dry and wet seasons (Fig. 2). This was particularly clear in 1993. The rain began to fall in late May while the $\delta^{18}O$ became lighter only in July. Similarly, when the rain stopped in October, the $\delta^{18}O$ did not become heavier until at least December. The cases for the transition in late 1992, late 1994, and early 1995 were not as strong but were consistent with similar time lags. The estimated residence time for water in Nanwan is about 40 days [53]. This 1- to 1.5-month delay would probably be caused by the time needed to replace the bay water with lighter $\delta^{18}O$ water during the wet season.

3.2. Inferred $\delta^{18}O_{sw}$ from modern coral

Coral $\delta^{18}O$ is affected by both local $\delta^{18}O_{sw}$ and SST and the first-order equation can be expressed as:

$$\delta^{18}O_{coral} - \delta^{18}O_{sw} = a + b \times \mathrm{SST}. \quad (1)$$

We have calibrated this relationship using our measured $\delta^{18}O_{coral}$ (Fig. 3) and the nuclear power plant's intake water temperature monitoring record for 1989–1990. For $\delta^{18}O_{sw}$, we used the mean values 0.07‰ and 0.30‰, respectively, for wet and dry seasons measured for 1995 seawater whose rainfall of 2099 mm/yr is similar to those of 1989–1990. The resulting equation is:

$$\delta^{18}O_{coral} - \delta^{18}O_{sw} = -0.771 - 0.180 \times \mathrm{SST}.$$
$$R^2 = 0.94 \quad (2)$$

If we had followed the usual practice of simply using the annual mean $\delta^{18}O_{sw}$, the fitting would have given a higher sensitivity of 0.247‰/°C instead, which is an artifact. Note that the range of this sensitivity determined before in many studies was 0.18–0.25. The common practice used in these studies [26–28,54] assumed a constant annual mean value for $\delta^{18}O_{sw}$. We suggest that a careful case by case reexamination should be done to obtain the correct sensitivity instead of simply taking the grand average of the set because many studies might require the use of separate seasonal values for $\delta^{18}O_{sw}$. We believe that

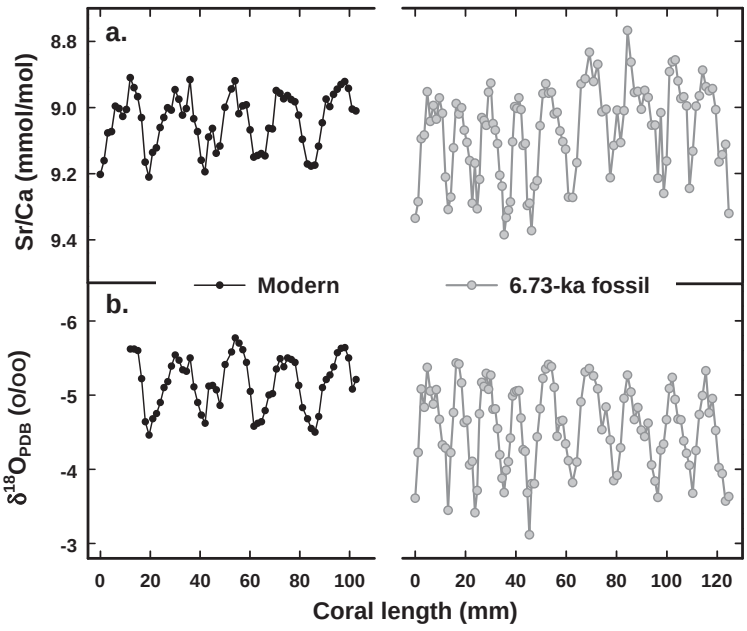

Fig. 3. The monthly records of skeletal (a) Sr/Ca and (b) δ^{18}O in a modern coral head *P. lutea* from 1989 to 1993 (solid circles and black lines; most data from Shen et al. [16]) and in a mid-Holocene *Porites* coral (gray lines with gray circles). Seasonal variations of Sr/Ca are caused by SST. However, the seasonal anomalies of coral δ^{18}O profiles are composite; about 80% is contributed by SST and the other by precipitation for the modern coral (see text).

the resulting sensitivity is closer to the low end of the present range (i.e. 0.18), consistent with the one, 0.18‰/°C, established during drought years for *Porites* corals from Orpheus Island, central Great Barrier Reef [18,28].

The relationship of coral *P. lutea* Sr/Ca–SST used here was established by Shen et al. [16] and written as:

$$D = 1.2054 - 0.005901 \times \mathrm{SST}, \quad (3)$$

where D is the distribution coefficient, defined as $D = \mathrm{Sr/Ca_{coral}}/\mathrm{Sr/Ca_{sw}}$. Eq. (3) can be rearranged as $\mathrm{SST} = (1.2054 - D)/0.005901$. Substitution of this relation into Eq. (2) yields:

$$\delta^{18}\mathrm{O_{sw}} = \Delta\delta^{18}\mathrm{O} = 37.54 + \delta^{18}\mathrm{O_{coral}} - 30.50 \times (\mathrm{Sr/Ca_{coral}}/\mathrm{Sr/Ca_{sw}}). \quad (4)$$

Here $\delta^{18}\mathrm{O_{sw}}$ represents the implied isotopic composition of seawater at the time of growth of the coral skeleton, which is calculated as the residual δ^{18}O or $\Delta\delta^{18}$O for the coral δ^{18}O record after removing the temperature component.

$\Delta\delta^{18}$O can be determined from Eq. (4), if coral Sr/Ca and δ^{18}O are both measured and $\mathrm{Sr/Ca_{sw}}$ is known. Five-year monthly resolved coral skeletal δ^{18}O and Sr/Ca records from 1989 to 1993 are plotted in Fig. 3 and modern Nanwan $\mathrm{Sr/Ca_{sw}}$ is 8.551 mmol/mol [16]. Applying Eq. (4) to this dataset, we can infer Nanwan $\delta^{18}\mathrm{O_{sw}}$ for this period (Fig. 4). Synchroneity between low $\Delta\delta^{18}$O and high SST indicates that the occurrence of depleted $\delta^{18}\mathrm{O_{sw}}$ was from the late spring to late summer. A direct comparison of seasonal oxygen isotopic variation between the calculated $\Delta\delta^{18}$O and the measured $\delta^{18}\mathrm{O_{sw}}$ can be made for the drought year of 1993, from which no information has been used for the derivation of Eq. (2) or Eq. (4). The averages for the coral $\Delta\delta^{18}$O data of the dry and wet seasons were 0.32‰ and 0.15‰, respectively, which reproduce those for the measured $\delta^{18}\mathrm{O_{sw}}$ remarkably well (Fig. 4). The $\Delta\delta^{18}$O values for the other years were reasonable as the dry seasons typically had the inferred $\delta^{18}\mathrm{O_{sw}}$ between 0.3‰ and 0.4‰, and wet seasons had values lighter by 0.20‰.

The only unusual data were for spring of 1991. The $\Delta\delta^{18}$O seemed to show an offset toward a lighter value by 0.20‰ after February. The reason for the anomalous $\Delta\delta^{18}$O signal is that offshore surface sea-

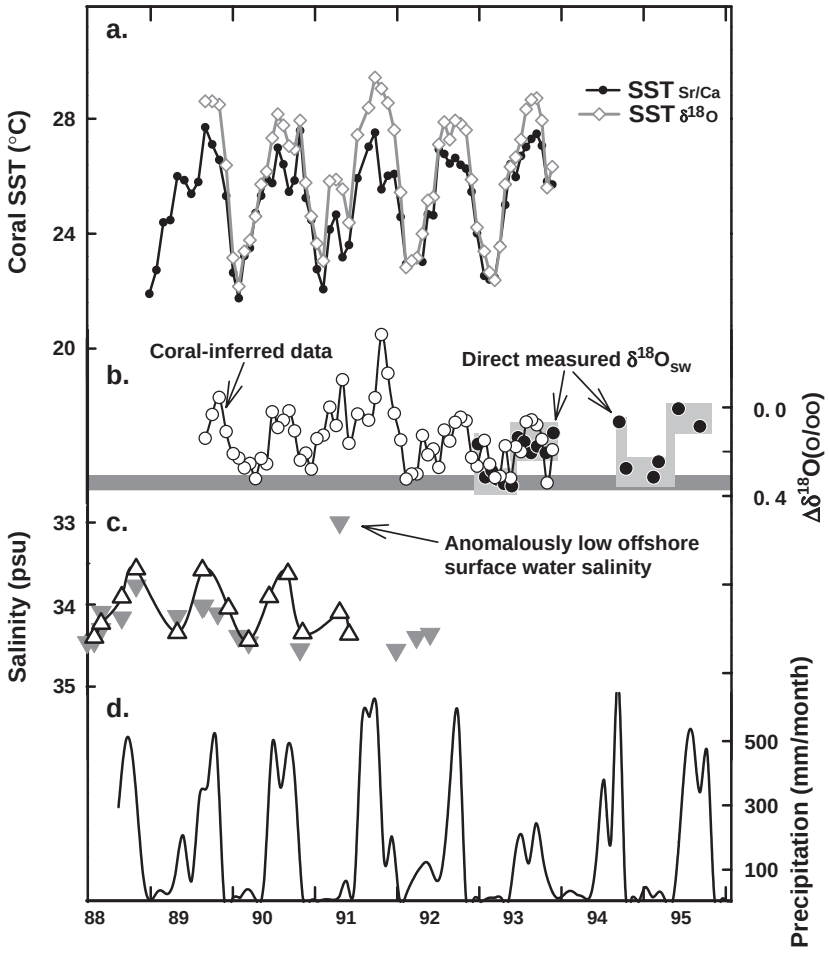

Fig. 4. (a) Calculated coral Sr/Ca (solid line with circles) and $\delta^{18}O$ temperatures (gray line with diamonds) of a modern *Porites* coral collected in Nanwan. Comparison among (b) coral residual $\delta^{18}O$ ($\Delta\delta^{18}O$, solid line with hollow circles) and direct measured Nanwan $\delta^{18}O_{sw}$ data (dusky region with solid circles), (c) seasonally measured salinity data for Nanwan water (1988–1991, open triangles) and offshore surface water (1988–1992, gray triangles) [40,55], and (d) monthly precipitation from 1988 to 1996. The variation of coral $\Delta\delta^{18}O$ is consistent with the occurrence of rainfall, except for the offset in 1991 spring, due to anomalously low salinity offshore surface water, which apparently had intruded into the Bay (see text). The dark gray horizon represents the averaged value of Nanwan $\delta^{18}O_{sw}$ in the dry season from coral and water data. Note that the coral samples are not calendared and the $\Delta\delta^{18}O$ record shown here is before age fitting.

water with an abnormally low salinity of 33.0 psu (Fig. 4c) (instead of 34.6 psu for the general dry season [40,55]) intruded into the bay, depleting $\delta^{18}O_{sw}$ while Nanwan received little rain in spring. It will be discussed later that the bay water consists of 25% offshore surface water and 75% upwelled water in the dry season. If such was the case in 1991, the salinity anomaly of 1.6 psu in the offshore surface water would cause a 0.4 psu decrease in Nanwan water and a 0.1–0.2‰ depletion in Nanwan $\delta^{18}O_{sw}$ in accord with a slope of 0.25–0.4‰/psu for the $\delta^{18}O_{sw}$–salinity relationship [19,23,53,56]. The depletion of both seawater and coral ^{18}O in the 1991 spring indicates that not only local but regional climatic conditions can affect hydrography in Nanwan.

3.3. Fidelity of coral Sr/Ca and $\delta^{18}O$ proxies for thermal and hydrological anomalies

Studies of Sr uptake in the coralline micro-structure have showed complicated micro-biogeochemical processes for elemental partitioning [31,32,34–37].

Physiological offsets from equilibrium of the coral Sr/Ca–SST and δ^{18}O–SST relationships in massive *Porites* corals have been reported [17,33,38]. Fallon et al. [57] analyzed Sr/Ca in three *Porites* corals collected from inshore, mid-shelf, and outer reef localities with different environmental stresses in the central Great Barrier Reef. They found a temperature variation of ~ 2 °C, within the analytical uncertainty, between three Sr/Ca–SST calibrations. It suggests that the influence of coral physiology may cause a possible temperature bias of 2 °C or less. Despite the fact that past seawater Sr/Ca variation in the Holocene cannot be absolutely mirrored in foraminiferal records [58], modeling studies suggest that seawater Sr/Ca could have changed with a 1–3% decrease in the last 15 ka [59], corresponding to a bias of 2–6 °C for the coral Sr thermometer.

The dispersion among coral Sr/Ca–SST calibrations and oceanic chemical evolution lead to uncertainties in the absolute coral Sr inferred temperature. Fortunately, the slopes of the worldwide calibration equations are similar [16,19,38]. There is no significant difference (*t*-test, $p=0.05$) between two new Sr/Ca–SST thermometers for 400-yr-old *Porites* corals collected from Nanwan and an offshore island Lutao, southwestern Taiwan [60], and our previous ones calibrated with 20-yr-old coral heads [16]. Consistency among the sensitivities of coral Sr thermometers suggests that the relative variation, like seasonal anomalies, addressed in the fossil corals is a reliable reflection of relative temperature.

Our resulting sensitivity of the δ^{18}O–SST calibration is consistent with the one, 0.18‰/°C, established by the Australian National University group [18,28]. However, a discrepancy between intercepts in the two equations are observed, probably due to different $\delta^{18}O_{sw}$ conditions and/or coral physiology [33,38]. Metabolic effects seem to not be serious when combining the empirical Sr/Ca–SST and δ^{18}O–SST relationships to reconstruct seawater hydrological anomalies [18–22]. Morimoto et al. [23] presented biweekly precise coral and in situ seawater data to demonstrate that the $\delta^{18}O_{sw}$ and salinity anomalies during the 1997–1998 El Niño can be deconvolved from Palau corals, even though the hydrological signals are only 0.2–0.5‰. Although precipitation brought about seasonal $\delta^{18}O_{sw}$ variations of 0.15–0.34‰ in Nanwan, only accounting for ~ 20% of the total annual coral δ^{18}O range (Fig. 4), we can resolve this change in precipitation. Previous studies and our observations suggest that the influence of the physiological effect is not significant for deciphering seawater thermal and hydrological anomalies with massive *Porites* corals.

3.4. Correlation between present precipitation and seawater $\delta^{18}O$ in Nanwan

The shifts of $\delta^{18}O_{sw}$ towards lighter values in the wet season is caused by the rain which is depleted in ^{18}O relative to seawater. The precipitation should, therefore, be expected to correlate with the shift in $\delta^{18}O_{d-w}=\delta^{18}O_d$ (dry season) $-\delta^{18}O_w$ (wet season). In Fig. 5 we plot the $\delta^{18}O_{d-w}$ for the 3 yr (1993–1995) when directly measured data for seawater samples were available and the 3 yr (1991–1993) when coral data were used to infer them after first removing the SST influence. Since the seawater and coral datasets generally agree with each other and essentially

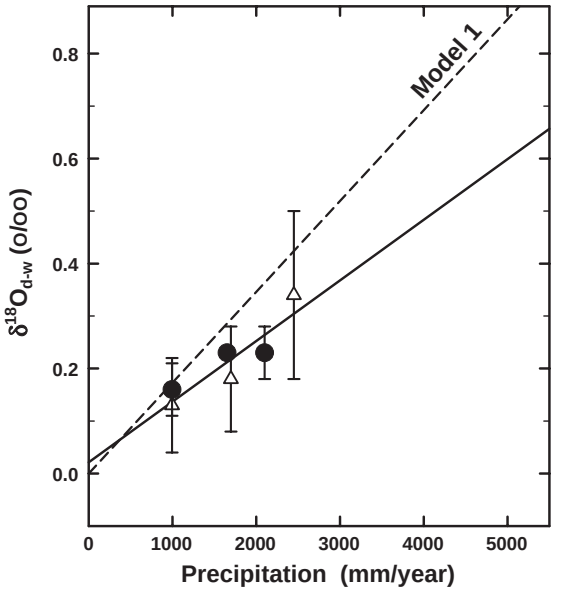

Fig. 5. The relationship between seasonal difference of seawater δ^{18}O ($\delta^{18}O_{d-w}$) and annual precipitation. Both measured (circles) and coral-inferred (triangles) data are used to build up the regression line. The dashed black line (Model 1) is predicted based on the Sr/Ca–salinity model, δ^{18}O–salinity diagram and assumption that offshore surface water δ^{18}O in wet seasons varies with rainfall.

coincide in 1993, we can fit a correlation line through all six data points to obtain:

$$\delta^{18}O_{d-w} = 0.02 + 1.16 \times 10^{-4} \times P \quad R^2 = 0.83, \tag{5}$$

where P is annual precipitation (mm/yr). In order to evaluate the applicability of this relationship, we need to better understand the mixing process of different water masses in Nanwan Bay that controls the salinity and the oxygen isotopic composition.

3.5. Hydrographic modeling of present seawater $\delta^{18}O$–precipitation relation

3.5.1. Mixing model

Here we invoke a mixing model which may be used to derive the mixing ratio of the three main sources for the Nanwan water: the surface seawater from the Luzon Channel that flows over the seamount, the upwelled seawater coming from a depth of 100–200 m through the canyon south of the bay, and the freshwater input, which is significant only in the wet season. The freshwater comes from the rain falling directly in the bay and from runoff and submarine ground water discharge from the small watershed whose size roughly equals that of the bay (Fig. 1). A simple mixing model employs steady-state mass balances of water, Sr/Ca and salinity in the mixing of the three endmembers. The model is based on hydrographic measurements at three stations along a transect from the coastal region immediately outside Nanwan to a station in 2000 m deep water 250 km to the south, where the depth profiles for salinity, temperature, $\delta^{18}O_{sw}$, and Sr/Ca were determined. In addition, we have also measured Sr/Ca and $\delta^{18}O$ of the runoff [52]. The chemical properties of Nanwan water and three water masses are listed in Table 1.

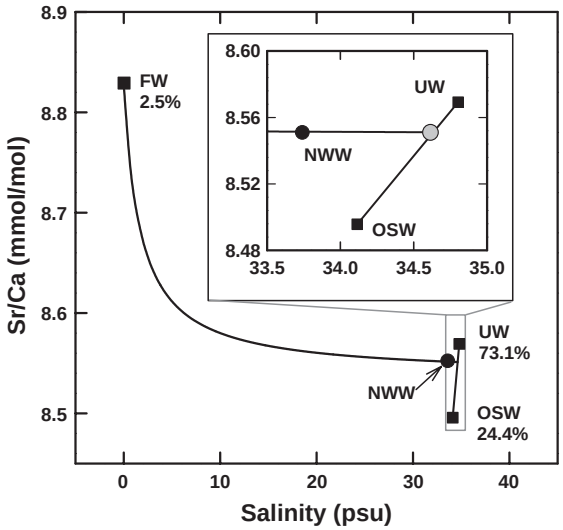

Fig. 6. Modeling the waters' mixing in Nanwan Bay using a Sr/Ca–salinity diagram [53]. Suppose the coastal water of Nanwan Bay (NWW, solid circle) is stoichiometrically mixed by three endmembers, freshwater (FW), upwelled water (UW) and offshore surface water (OSW) (solid squares). For the case of the 1994 wet season, the percentages of those endmembers are: upwelled water 73.1%, offshore surface water 24.4%, and freshwater 2.5%. In the dry season the coastal water is mixed by only upwelled and offshore surface waters. The value of coastal seawater Sr/Ca will thus be 8.551 mmol/mol (gray circle in the inset enlarged plot), the same as the annual mean (solid circle).

Using the properties of the three components of water in Nanwan, we plot the expected mixing relationship between Sr/Ca and salinity in Fig. 6. Since the Sr and Ca concentrations of freshwater are much lower than that of seawater, the Sr/Ca of Nanwan water is essentially controlled by the mixing between upwelled and surface waters. The measured Sr/Ca of the mixture and its two end members thus immediately gives the mixing proportion between the two seawaters. The upwelled component is thus found to

Table 1
Sr/Ca, salinity and $\delta^{18}O$, of Nanwan water and its three endmembers[a]

Water mass	Sr/Ca (mmol/mol)	Salinity (psu)		$\delta^{18}O$ (‰)	
		Dry season	Wet season	Dry season	Wet season
Nanwan water	8.551	34.4–34.6	33.74	0.28–0.32	0.08
Endmember components					
Freshwater	8.827	0	0	− 8.38	− 8.38
Offshore surface water	8.496	34.60	34.12	0.25	0.10
Upwelled water	8.569	34.80	34.80	0.36	0.36

[a] Data from [53].

contribute 75%. On the other hand, the salinity difference between the surface and the upwelled waters is small when compared to the huge contrast relative to that of the freshwater. The addition of freshwater in the wet season shifts the mixture point along the constant Sr/Ca line towards the direction of low salinity. The contribution of freshwater to Nanwan in the wet season of 1994 was thus estimated to be about 2.5%. This modeling effort is described in full detail elsewhere [53]. Here we only outline how we use the mixing process to predict the relationship between $\delta^{18}O_{d-w}$ and precipitation.

3.5.2. Modeled $\delta^{18}O_{d-w}$–precipitation relation

In the following we use a step by step mixing process to derive the $^{18}O_{d-w}$–precipitation relationship in the Nanwan. In Fig. 7, we plot the $\delta^{18}O$ against salinity of various water masses for 1994. In the dry season, the mixing at a proportion of 3:1 between upwelled and surface waters produces a $\delta^{18}O_{sw}$ of 0.33‰, which is consistent with the observed and implied values of 0.30–0.35‰ from Nanwan water and corals shown in Fig. 4. In the wet season, the offshore surface water became ^{18}O-poor and less salty (Fig. 4c), reflecting the effect of rainfall on regional hydrography.

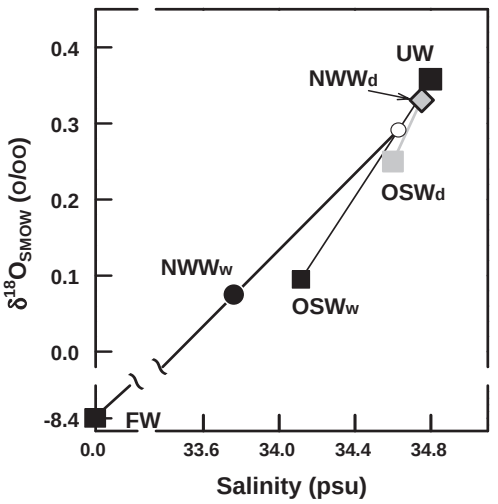

Fig. 7. Simulation of the alteration of the $\delta^{18}O$ value for the coastal water in different seasons using the $\delta^{18}O$–salinity diagram based on the mixing model illustrated by the Sr/Ca–salinity diagram shown in Fig. 6. In dry seasons the value of Nanwan $\delta^{18}O_{sw}$ is 0.33‰ (gray diamond) through the mixing of upwelled (UW, solid cube) and offshore surface waters (OSW_d, gray cube). In wet seasons the value of $\delta^{18}O$ of coastal water will drift from the one (hollow circle) of mixing by UW and offshore water (OSW_w) towards the one of freshwater (solid line). For the 1994 case, the modeled value of $\delta^{18}O_{sw}$ in the bay is 0.08‰ (NWW_w, solid circle).

The mixing of the upwelled water, which had the same composition as in the dry season, and the offshore surface seawater, which was less saline and more depleted in ^{18}O, produces a seawater mixture that has a somewhat lower $\delta^{18}O_{sw}$ of 0.29‰ (Fig. 7). The addition of freshwater in Nanwan further shifted the $\delta^{18}O_{sw}$ of the final mixture to 0.07‰, thus resulting in a $\delta^{18}O_{d-w}$ of 0.26‰ for a year (1994) with 1651 mm precipitation. In other words, the shift in $\delta^{18}O$ of the offshore water in the wet season accounts for a 0.04‰ decrease of the bay water isotopic composition, while the local rainfall accounts for a 0.22‰ decrease. Therefore, the effect of precipitation on the $\delta^{18}O_{sw}$ of the bay is calculated to be 1.33×10^{-4}‰ mm^{-1}, which is controlled by the relative contributions of seawaters and freshwater. Because the offshore surface water comprises ~ 25% of the Nanwan water, the seasonal difference in $\delta^{18}O_{sw}$ of the bay can be expressed as:

$$\delta^{18}O_{d-w} = 25\% \times \left(\delta^{18}O_{d-w}\right)_{off} + 1.33\times10^{-4}\times P, \quad (6)$$

where $(\delta^{18}O_{d-w})_{off}$ is the seasonal difference of $\delta^{18}O$ for offshore surface water. As the $(\delta^{18}O_{d-w})_{off}$ value is difficult to predict and the relative contributions of different endmembers may vary over the geological time, we have considered possible scenarios in two models. For Model 1, we assume that the precipitation outside the bay also equals P and the value of its $\delta^{18}O$ is − 8.38 (± 0.48)‰ [61]. The hydrographic profiles observed off the southern tip of Taiwan in summer [62] indicate a mixed layer depth of about 50 m. Thus the value of $(\delta^{18}O_{d-w})_{off}$ may be expressed as $1.6\times10^{-4}\times P$, which is plugged into Eq. (6) to produce the relationship:

$$\delta^{18}O_{d-w} = 1.73\times10^{-4}\times P. \quad (7)$$

Note that this line passes through all data within their 1σ bars except that for 1995 whose uncertainty may be under-estimated because there were only two measurements for the wet season (Fig. 2). Basically, the observed correlation can be explained by the hydrographic mixing model (Fig. 5).

The different trends of freshwater dilution observed in Nanwan Bay and the offshore region shown in Fig. 7 may be attributed to the slight difference between $\delta^{18}O$ values of the local rain and the offshore precipitation. Besides, during the isotopic change of offshore water from the dry season to the wet season it may have experienced not only freshwater dilution but probably also evaporation, which tends to enrich salinity more efficiently than the heavier oxygen isotope in the tropics [63].

3.6. Chemical and isotope records in fossil coral

3.6.1. Sr/Ca and $\delta^{18}O$ records

Nine-year records of skeletal Sr/Ca and $\delta^{18}O$ of a 6.73-ka fossil sample are illustrated in Fig. 3. The seasonal extremes of Sr/Ca shifted from 8.9 to 9.4 mmol/mol in years Y1–Y5 to 8.8–9.2 mmol/mol in years Y6–Y9. This trend was not observable in the $\delta^{18}O$ record, ranging from − 5.2‰ to − 3.8‰. Both amplitudes are larger than their counterparts in modern coral (Fig. 3). In addition, the mean values of the two sets of records have significant offsets from modern values.

3.6.2. Sr-inferred SST anomaly

In the first 4 yr Y1–Y4 within the 6.73-ka window, the inferred range of seasonal SST variations was 6.7 ± 0.7 °C (Fig. 8). From the winter of Y5 onward, the annual mean SST in Nanwan climbed 1° higher. The amplitude of seasonal variations was 6.7 ± 0.5 °C in years Y6–Y9, similar to the range in Y1–Y4. The mean SST for the 9-yr window was 24.4 °C, which was 0.5 °C cooler than the present, assuming the seawater Sr/Ca in Nanwan did not differ significantly from today. Instrumental and coral inferred data give the modern annual temperature range of 5.8 ± 0.5 °C (Fig. 4a) [52,60], which means the average seasonality (6.7 °C) at the 6.73-ka window shown in Fig. 8 was 16% larger than the present. This feature is expected qualitatively from Milankovitch cycle since at 9 ka, earth's perihelion fell in the northern summer and aphelion fell in the northern winter, which caused a 10% larger swing of northern hemisphere solar

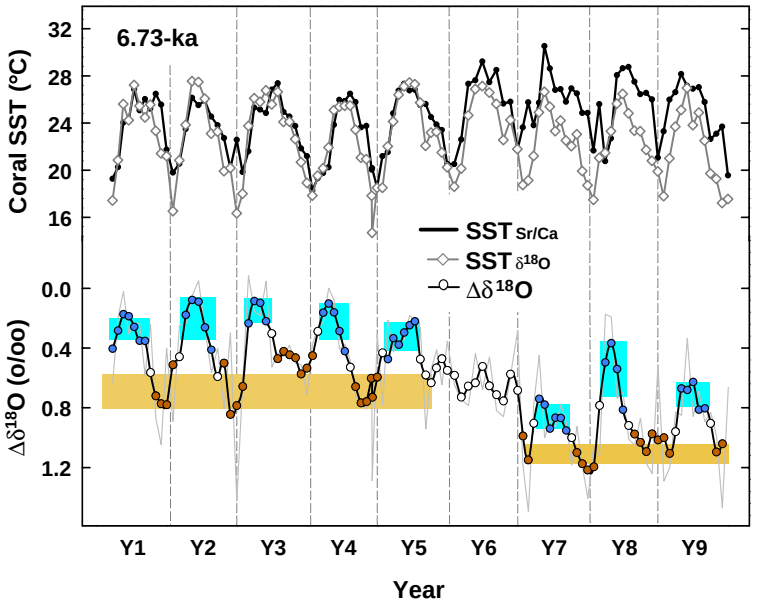

Fig. 8. Calculated coral Sr/Ca (higher solid line with black circles), $\delta^{18}O$ temperatures (gray line with diamonds) and $\Delta\delta^{18}O$ (lower thin gray line) for a 6.73-ka *Porites* coral. Note Sr/Ca and $\delta^{18}O$ data were measured with two different adjacent cubes for each horizon of the fossil coral. A three-point-averaged $\Delta\delta^{18}O$ line (lower solid line with hollow circles) is calculated here to remove the possible asynchronicity between the two parallel subsamples. The averaged $\Delta\delta^{18}O$ values in dry seasons of two spans Y1–Y5 and Y7–Y9 are calculated with dark red symbols (1σ) and shown as brown regions, and wet seasons for these years with blue symbols as cyan rectangles. Note that a lead of low $\Delta\delta^{18}O$ over the Sr/Ca-inferred high SST with 2–3 subsample points is observed for years Y1, Y3–Y5 and Y8.

insolation at 6–7 ka [64–66]. On the other hand, the SST seasonality is also dependent on local circulation, which may have magnified the seasonal temperature response.

3.6.3. Inferred $\delta^{18}O_{sw}$ anomaly

The $\Delta\delta^{18}O$ record within the 9-yr window at 6.73 ka is depicted in Fig. 8. The enriched $\delta^{18}O$ for the dry seasons, measured from seawaters and inferred from modern corals, characterizes the seawater without the freshwater contribution (Figs. 2 and 4). When the volume of the ice cap was still slightly larger than the present, $\delta^{18}O_{sw}$ was expected to be 0–0.1‰ heavier than that of today in the mid-Holocene, [67–69]. The values of the inferred $\delta^{18}O_{sw}$ for the dry seasons are larger than those of the present day by 0.3‰ for years Y1–Y5. The increase is larger than the ice volume effect (Fig. 8). The enrichment in ^{18}O could be caused either by the different water conditions over the Holocene or by physiology discrepancies between modern and fossil coral colonies, which can probably bias the values of intercepts in the Sr/Ca–SST and $\delta^{18}O$–SST equations [19,22,38].

Three features are found in the inferred $\delta^{18}O_{sw}$ anomaly record (Fig. 8). (1) The rather constant $\Delta\delta^{18}O$ for the dry seasons in Y1–Y5, increased through Y6, and reached a new level 0.40‰ heavier in Y7–Y9. (2) The inferred seasonal $\delta^{18}O_{sw}$ differences were 0.45 ± 0.17‰ in Y1–Y5 and 0.37 ± 0.14‰ in Y7–Y9. The seasonal difference in Y6 is not clear. Excluding Y6, we calculate an average seasonal difference of 0.42 ± 0.11‰. (3) For the years of Y2, Y7 and Y9, a close synchroneity between phases of $\Delta\delta^{18}O$ and coral Sr/Ca-inferred SST is consistent with those observed from modern records. Instead, for years of Y1, Y3–Y5 and Y8, the $\Delta\delta^{18}O$ values became progressively negative in the early spring and then reached minima. The low $\Delta\delta^{18}O$ and high SST data were asynchronous with 2–3 subsample points for these years.

A simple extrapolation of the relationship between precipitation and the seasonal difference ($\delta^{18}O_{d-w}$) obtained from the modern data (Eq. (5)), the 2 times larger seasonal difference in $\delta^{18}O$ (0.42 ± 0.11‰) would yield a rainfall of 1500–4400 mm/yr, which is 1.5 times as high as the modern values. A precipitation of 1700–2900 mm/yr would be predicted using Model 1, lower than that calculated by Eq. (5). Before jumping into any conclusions, the influence of a different hydrographic condition in the mid-Holocene should be carefully evaluated.

3.7. Paleo-conditions

3.7.1. Magnitude of precipitation

Model 1 as represented by Eq. (7) may be applicable for the modern condition. Instead, the effects of tectonic evolution, sea level change and hydrographic alteration on the seawater fluxes must be considered for paleo-conditions. An average tectonic uplift rate of 3.9 mm/yr in the Nanwan area [48] suggests that there could have been a 26 m change in elevation over 6.7 ka, which is substantial for a mean water depth of only 63 m in the bay. The fraction of the local freshwater contribution could have been diminished by 41% because the bay reservoir was larger than the present by a factor of 26/63. Although the contributions of the two seawater endmembers in the mid-Holocene are difficult to assess, we have investigated the sensitivity of the relationship to changes in relative contribution of the endmembers in Model 2. If the magnitude of upwelled water did not vary significantly and only the flux of offshore surface water was affected by relative sea level change during the mid-Holocene, the relative contributions of upwelled water and offshore surface water would be estimated as 44% and 56%, respectively. Accordingly, Eq. (6) can be expressed as:

$$\delta^{18}O_{d-w} = 56\% \times \left(\delta^{18}O_{d-w}\right)_{off} + (1 - 41\%) \times 1.33 \times 10^{-4} \times P, \quad (8)$$

$$= 0.90 \times 10^{-4} \times P + 0.79 \times 10^{-4} \times P, \quad (9)$$

$$= 1.69 \times 10^{-4} \times P. \quad (10)$$

This relationship is not significantly different from that for Model 1, suggesting that the seasonal difference in $\delta^{18}O$ values of the bay water is not sensitive to change in topography of the bay. Using Model 2, we would translate the seasonal Nanwan water $\delta^{18}O$ shift into a precipitation of 1800–3000 mm/yr, ~ 20% higher than that of today (1500–2500 mm/yr) (Fig. 9). The abundance of spores in the pollen record recovered from lake sediments in Taiwan and the geochemical tracers shown in the deep sea sediments from the

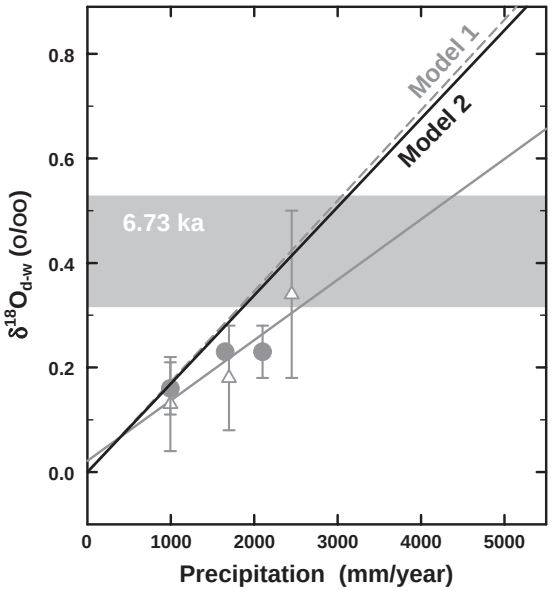

Fig. 9. Derived relationships between seasonal $\delta^{18}O_{sw}$ difference ($\delta^{18}O_{d-w}$) and annual precipitation at 6.73 ka by Model 2 (solid line), involving local tectonic activity and sea level change in the mid-Holocene. The range of seasonal anomalies of $\Delta\delta^{18}O$ recorded in a fossil *Porites* coral is shown as gray area. A regression line built with measured (circles) and modern coral-inferred (triangles) data is shown as a dark gray line, and Model 1 as a dashed dark gray line.

South China Sea both indicate a wet climatic condition [70], qualitatively consistent with our results mentioned above. The contributions of offshore surface water and freshwater for seasonal $\delta^{18}O_{sw}$ variation in Nanwan varied from 23:77 today (Eq. (6)) to 53:47 at 6.7 ka (Eq. (9)), when relative sea level was high and Nanwan was more open. The intrusive offshore surface water, therefore, contributed more substantial $\delta^{18}O_{sw}$ variability in Nanwan in the mid-Holocene. A summary of scenarios of Nanwan hydrographic conditions for Model 1 and Model 2 is given in Table 2.

3.7.2. Rainfall seasonality

The timing or phase of the seasonal cycle of rainfall may be inferred from the $\Delta\delta^{18}O$ record at the 6.73-ka window as illustrated in Fig. 8. The phase of the $\Delta\delta^{18}O$ pattern for years Y2, Y7 and Y9, is the same as present, suggesting a similar rainy season at those years. For years Y1, Y3–Y5 and Y8, the decrease of $\Delta\delta^{18}O$ preceded the increase of SST slightly. It suggests that the rainy season probably occurred from the early–mid-spring to mid-summer.

Possible forcing resulting in the early occurrence of the rainy season for the years of Y1, Y3–Y5 and Y8 is described as follows. The East Asian monsoon maximum shifted systematically southeastward in the past 10,000 yr [71]. The maximum precipitation was located at north-central China by 7 ka and the Yangtze River area in the mid-Holocene (5–7 ka). The findings were further supported by the record of desert/loess transitions [72]. These results indicate a stronger East Asian summer monsoon reaching latitudes north of its present position. Strengthened solar insolation in the mid-Holocene [64–66] might prompt large land–sea temperature contrast and a northward-shifted East Asian summer monsoon [73]. The early heating of the continent likely triggered an early onset of the rainy season in Taiwan. At the present time, the long-term record of the East Asian summer monsoon rainfall anomalies from interannual to centennial time scales exhibits a phase reversal between the Yangtze River valley and south China and Taiwan [74,75]. If a similar pattern prevailed in the mid-Holocene, the early northward march of the seasonal rainband to central China would probably suppress the rainfall

Table 2
Summary of scenarios of Nanwan hydrographic conditions for Model 1 and Model 2

Hydrograhic condition	Water mass[a]	Model 1	Model 2
Averaged bay depth		37 m (present)	63 m (6.73 ka)
Relative sea level		0 m	− 26 m
Percentages of water masses in dry seasons	FW	0%	0%
	OSW	25%	56%
	UW	75%	44%
Percentages of water masses in wet seasons	FW	2.5%[b]	F%; decreased with a factor of 26/63 relative to modern condition
	OSW	24.4%[a]	$56/(1-F/100)$%
	UW	73.1%[a]	$44/(1-F/100)$%
Contribution of water masses for seasonal $\delta^{18}O_{sw}$[c]	FW	77%	47%
	OSW	23%	53%

[a] FW: freshwater; OSW: offshore surface water; UW: upwelled water.
[b] A case of the 1994 wet season with 1651 mm precipitation.
[c] Based on an assumption that the amounts of precipitation in and out of the bay are the same.

after mid-summer as recorded in fossil coral in Nanwan (Fig. 8). It is suggestive that the early occurrence of the Mei-Yu rainfall and the suppression of summer rainfall likely resulted in the phase shift of the rainy season at 6.73 ka. A strong zonal SST gradient and enhanced summer monsoon in the mid-Holocene [70–72] could possibly bring about a heavy early-season precipitation in the western tropical Pacific.

It is noted that the change in seasonality may have been caused by non-local effects. The record from 1991 (Fig. 4) indicates that an anomalously low salinity water outside the bay may bring about the occurrence of depleted Nanwan $\delta^{18}O_{sw}$ in spring. A similar event may have happened in years of Y1, Y3–Y5 and Y8. More modern hydrological observations, coral data and hydrographic models may sufficiently address this issue in further studies.

3.7.3. $\Delta\delta^{18}O$ in dry seasons

The $\Delta\delta^{18}O$ value in the dry seasons of years Y7–Y9 was enriched by 0.4‰ over that of years Y1–Y5. Based on modern observations (Figs. 2 and 3) and a water mixing model [53], the variation of $\Delta\delta^{18}O$ value in the dry season is only attributed to offshore surface water and upwelled water. The 0.4‰ enrichment in Nanwan water ^{18}O was probably not just attributed to only local SST rise. We argue that it might be caused by a regional SST increase. Gagan et al. [18] proposed an evaporative enrichment of 0.5‰ in seawater ^{18}O can be driven by 1 °C temperature increase in the southwestern Pacific at 5.35 ka according to modern observations and a GCM calculation [76]. A two-degree rise in SST, addressed in the Sr/Ca record, in the western Pacific area can cause 0.5‰ enrichment for Nanwan $\delta^{18}O_{sw}$, close to the observed 0.4‰ offset, if the contribution of offshore surface water was 56% (Model 2) in Nanwan. The $\Delta\delta^{18}O$ value in the fall and winter of year Y3 was 0.2‰ depleted than that of the other years in Y1–Y5, suggesting an episode of a remarkable local and/or regional winter rainfall, or an intrusion of low salinity offshore surface water.

4. Conclusions and recommendations

In this research we measured directly the seasonal $\delta^{18}O_{sw}$ offset in Nanwan, a semi-enclosed bay, and established its correlation with precipitation. For the coastal water, the seasonal $\delta^{18}O_{sw}$ difference was about 0.2‰, which is registered in the coral skeleton. This hydrological signal contributed to only 20% of the seasonal variation of coral $\delta^{18}O$. Using hydrological models we also succeeded in constructing a theoretical relationship between seasonal $\delta^{18}O_{sw}$ difference and precipitation and demonstrated that coral Sr/Ca and $\delta^{18}O$ records can be used as a quantitative proxy for the past precipitation.

Taking advantage of this method, we reconstructed the past precipitation and climatic conditions at 6.73 ka. The residual $\delta^{18}O$ records suggest an annual rainfall of 1800–3000 mm/yr, 20% higher than that of today. We speculated that the magnitude of precipitation and the onset of the rainfall season might be influenced by strengthened solar insolation and an enhanced Asian summer monsoon. Although we have carefully examined the applicability of combining coral Sr/Ca and $\delta^{18}O$ records as a paleo-precipitation proxy, there are still many uncertainties in the assumptions made in this study, including the mixing of water masses, sea level changes, monsoon intensities and coastal circulation conditions. The current dataset is still insufficient for reconstructing detailed precipitation history. More observational records and modeling simulations are needed to understand the mechanism of teleconnection between Asian monsoons and/or possible ENSO fluctuations and their induced precipitation characteristics.

In view of the complications involved in reconstructing climatic conditions, especially precipitation, we suggest that the appropriate sites should meet the following criteria in the next generation of similar studies:

(1) The local tectonics must be simple with little change vertically (uplift or subsidence) or horizontally (fault movement).
(2) The local hydrography must be simple with as little upwelling as possible.
(3) The reservoir must be sensitive to rainfall. Namely, the rainfall should be the major contributor to the changes and its rate of change is rapid to minimize the residence time uncertainties. Yet the reservoir must exchange readily with seawater from the open ocean to minimize local variations and to ensure rapid mixing.

(4) If precipitation is the main goal, we may consider a site close to the equator where SST variation is small.

Combining these, we suggest that a better site for such a study may be corals grown inside a small shallow lagoon formed around the caldera of a submerged but stabilized extinct volcano. It should be close to the equator and an isolated small peak surrounded by very deep ocean. The "democracy" reef (117°E, 15°N) in the South China Sea west of Luzon Island may be such a site.

Acknowledgements

We thank Chang-Feng Dai of the Oceanography Institute of National Taiwan University for his guidance in sample collection. Discussion with Chia Chou, Kuo-Yen Wei and Glenn Unruh was helpful. C.-C. Shen and T. Lee thank the researchers at Lamont Doherty Earth Observatory, especially Wallace Broecker, for gracious hospitality and insightful comments during their visit in late 1997. Constructive and comprehensive reviews by M. Gagan and one anonymous reviewer significantly improved this paper. This research was supported by R.O.C. Taiwan NSC grants (92-2116-M-002013, 93-2116-M-002036 and 94-2752-M-002-011-PAE to CCS, 93-2611-M-008003 to KKL, 92-2116-M-001015 to CHW, and 93-2611-M-291001 to HJL) and a USA NSF grant (0214041 to RLE).

References

[1] CIESIN, Gridded Population of the World GPW, Version 2. Center for International Earth Science Information Network, Columbia University, Palisades, NY., 2000. Available at http://sedac.ciesin.columbia.edu/plue/gpw.

[2] S.R. Epstein, R. Buchsbaum, H.A. Lowestam, H.C. Urey, Revised carbonate–water isotopic temperature scale, Bull. Geol. Soc. Am. 64 (1953) 1315–1326.

[3] J.N. Weber, P.M.J. Woodhead, Temperature dependence of oxygen-18 concentration in reef coral carbonates, J. Geophys. Res. 77 (1972) 463–473.

[4] J.E. Cole, G.T. Shen, R.G. Fairbanks, M. Moore, The Southern Oscillation recorded in the δ^{18}O of corals from Tarawa Atoll, Paleoceanography 5 (1990) 669–683.

[5] J.E. Cole, R.G. Fairbanks, G.T. Shen, Recent variability in the Southern Oscillation: isotopic results from a Tarawa Atoll coral, Science 260 (1993) 1790–1793.

[6] B.K. Linsley, R.B. Dunbar, G.M. Wellington, D.A. Mucciarone, A coral-based reconstruction of Intertropical Convergence Zone variability over Central America since 1707, J. Geophys. Res. 99 (1994) 9977–9994.

[7] A.W. Tudhope, G.B. Shimmield, C.P. Chilcott, M. Jebb, A.E. Fallick, A.N. Dalgleish, Recent changes in climate in the far western equatorial Pacific and their relationship to the Southern Oscillation: oxygen isotope records from massive corals, Papua New Guinea, Earth Planet. Sci. Lett. 136 (1995) 575–590.

[8] C.D. Woodroffe, M.R. Beech, M.K. Gagan, Mid-late Holocene El Niño variability in the equatorial Pacific from coral microatolls, Geophys. Res. Lett. 30 (2003), doi:10.1029/2004GL019972.

[9] H.V. McGregor, M.K. Gagan, Western Pacific coral delta O-18 records of anomalous Holocene variability in the El Niño-Southern Oscillation, Geophys. Res. Lett. 30 (2004), doi:10.1029/2002GL015868.

[10] F.E. Urban, J.E. Cole, J.T. Overpeck, Influence of mean climate change on climate variability from a 155-year tropical Pacific coral record, Nature 407 (2000) 989–993.

[11] A.W. Tudhope, C.P. Chilcott, M.T. McCulloch, E.R. Cook, J. Chappell, R.M. Ellam, D.W. Lea, J.M. Lough, G.B. Shimmield, Variability in the El Niño-Southern Oscillation through a glacial–interglacial cycle, Science 291 (2001) 1511–1517.

[12] K.M. Cobb, C.D. Charels, H. Cheng, R.L. Edwards, El Niño/Southern Oscillation and tropical Pacific climate during the last millennium, Nature 424 (2003) 271–276.

[13] C.D. Charles, K.M. Cobb, M.D. Moore, R.G. Fairbanks, Monsoon–tropical ocean interaction in a network of coral records spanning the 20th century, Mar. Geol. 201 (2003) 207–222.

[14] J.W. Beck, R.L. Edwards, E. Ito, F.W. Taylor, J. Recy, F. Rougerie, P. Joannot, C. Henin, Sea-surface temperature from coral skeletal strontium/calcium ratios, Science 257 (1992) 644–647.

[15] M.T. McCulloch, M.K. Gagan, G.E. Mortimer, A.R. Chivas, P.J. Isdale, A high-resolution Sr/Ca and δ^{18}O coral record from the Great Barrier Reef, Australia, and the 1982–1983 El Niño, Geochim. Cosmochim. Acta 58 (1994) 2747–2754.

[16] C.-C. Shen, T. Lee, C.-Y. Chen, C.-H. Wang, C.-F. Dai, L.-A. Li, The calibration of D[Sr/Ca] versus sea surface temperature relationship for *Porites* corals, Geochim. Cosmochim. Acta 60 (1996) 3849–3858.

[17] C.A. Alibert, M.T. McCulloch, Strontium/calcium ratios in modern *Porites* corals from the Great Barrier Reef as a proxy for sea surface temperature: calibration of the thermometer and monitoring of ENSO, Paleoceanography 12 (1997) 345–363.

[18] M.K. Gagan, L.K. Ayliffe, D. Hopley, J.A. Cali, G.E. Mortimer, J. Chappell, M.T. McCulloch, M.J. Head, Temperature and surface–ocean water balance of the mid-Holocene tropical Western Pacific, Science 279 (1998) 1014–1018.

[19] M.K. Gagan, L.K. Ayliffe, J.W. Beck, J.E. Cole, E.R.M. Druffel, R.B. Dunbar, D.P. Schrag, New views of tropical paleoclimates from corals, Quat. Sci. Rev. 19 (2000) 45–64.

[20] T.M. Quinn, D.E. Sampson, A multiproxy approach to reconstructing sea surface conditions using coral skeleton geochemistry, Paleoceanography 17 (2002), doi:10.1029/2000PA000528.
[21] E.J. Hendy, M.K. Gagan, C.A. Alibert, M.T. McCulloch, J.M. Lough, P.J. Isdale, Abrupt decrease in tropical Pacific sea surface salinity at end of Little Ice Age, Science 295 (2002) 1511–1514.
[22] L. Ren, B.K. Linsley, G.M. Wellington, D.P. Schrag, O. Hoegh-Guldberg, Deconvolving the δ^{18}O seawater component from subseasonal coral δ^{18}O and Sr/Ca at Rarotonga in the southwestern subtropical Pacific for the period 1726 to 1997, Geochim. Cosmochim. Acta 67 (2002) 1609–1621.
[23] M. Morimoto, O. Abe, H. Kayanne, N. Kurita, E. Matsumoto, N. Yoshida, Salinity records for the 1997–98 El Niño from Western Pacific corals, Geophys. Res. Lett. 29 (2002), doi:10.1029/2001GL013521.
[24] M.K. Gagan, E.J. Hendy, S.G. Haberle, W.S. Hantoro, Post-glacial evolution of the Indo-Pacific Warm Pool and El Niño-Southern Oscillation, Quat. Int. 127 (2004) 127–143.
[25] T. Corrège, M.K. Gagan, J.W. Beck, G.S. Burr, G. Cabioch, F.L. Cornec, Interdecadal variation in the extent of South Pacific tropical waters during the Younger Dryas event, Nature 428 (2004) 927–929.
[26] T.A. McConnaughey, ^{13}C and ^{18}O isotopic disequilibria in biological carbonates: I. Patterns, Geochim. Cosmochim. Acta 53 (1989) 151–162.
[27] G.M. Wellington, R.B. Dunbar, G. Merlen, Calibration of stable oxygen isotope signatures in Galapagos corals, Paleoceanography 11 (1996) 467–480.
[28] M.K. Gagan, A.R. Chivas, P.J. Isdale, High-resolution climate records from corals using ocean temperature and mass-spawning chronometers, Earth Planet. Sci. Lett. 121 (1994) 549–558.
[29] S. de Villiers, B.K. Nelson, A.R. Chivas, Biological controls on coral Sr/Ca and δ^{18}O reconstructions of sea surface temperature, Science 269 (1995) 1247–1249.
[30] N. Allison, A.W. Tudhope, A.E. Fallick, Factors influencing the stable carbon and oxygen isotopic composition of *Porites lutea* coral skeletons from Phuket, South Thailand, Coral Reefs 15 (1996) 43–57.
[31] N. Allison, Comparative determination of trace and minor elements in coral aragonite by ion microprobe analysis, with preliminary results from Phuket, southern Thailand, Geochim. Cosmochim. Acta 60 (1996) 3457–3470.
[32] S.R. Hart, A.L. Cohen, An ion probe study of annual cycles of Sr/Ca and other trace elements in corals, Geochim. Cosmochim. Acta 60 (1996) 3075–3084.
[33] A.L. Cohen, S.R. Hart, The effect of colony topography on climate signals in coral skeleton, Geochim. Cosmochim. Acta 61 (1997) 3905–3912.
[34] N. Allison, A.A. Finch, S.R. Sutton, M. Newvill, Strontium heterogeneity and speciation in coral aragonite: implications for the strontium paleothermometer, Geochim. Cosmochim. Acta 65 (2001) 2669–2676.
[35] A.L. Cohen, G.D. Layne, S.R. Hart, P.S. Lobel, Kinetic control of skeletal Sr/Ca in a symbiotic coral: implications for the paleotemperature proxy, Paleoceanography 16 (2001) 20–26.
[36] A.L. Cohen, K.E. Owens, G.D. Layne, N. Shimizu, The effect of algal symbionts on the accuracy of Sr/Ca paleotemperatures from corals, Science 296 (2002) 331–333.
[37] A. Meibom, M. Stage, J. Wooden, B.R. Constantz, R.B. Dunbar, A. Owen, N. Grumet, C.R. Bacon, C.P. Camberlain, Monthly strontium/calcium oscillations in symbiotic coral aragonite: biological effects limiting the precision of the paleotemperature proxy, Geophys. Res. Lett. 30 (2003), doi:10.1029/2002GL016864.
[38] J.F. Marshall, M.T. McCulloch, An assessment of the Sr/Ca ratio in shallow water hermatypic corals as a proxy for sea surface temperature, Geochim. Cosmochim. Acta 66 (2002) 3263–3280.
[39] N. Allison, A.A. Finch, High-resolution Sr/Ca records in modern *Porites lobata* corals: effects of skeletal extension rate and architecture, Geochem. Geophys. Geosyst. 5 (2004), doi:10.1029/2004GC000696.
[40] J.-C. Su, T.-C. Hung, Y.-M. Chiang, T.-H. Tan, K.-H. Chang, K.-T. Shao, P.-P. Hwang, K.-T. Lee, C.-C. Huang, C.-Y. Huang, K.-L. Fan, S.-Y. Yeh, An ecological survey on the waters adjacent to the nuclear power plant in southern Taiwan, National Scientific Committee on Problems of the Environment, Academia Sinica, Taipei, Taiwan, ROC, 1979–91 (in Chinese).
[41] H.-J. Lee, S.-Y. Chao, K.-L. Fan, Y.-H. Wang, N.-K. Liang, Tidally induced upwelling in a semi-enclosed basin: Nanwan Bay, J. Oceanogr. 53 (1997) 467–480.
[42] H.-J. Lee, S.-Y. Chao, K.-L. Fan, Flood-ebb disparity of tidally induced recirculation Eddies in a semi-enclosed basin: Nanwan Bay, Cont. Shelf Res. 19 (1999) 871–890.
[43] H.-J. Lee, S.-Y. Chao, K.-L. Fan, T.-Y. Kuo, Tide-induced eddies and upwelling in a semi-enclosed basin: Nan Wan, Estuar. Coast. Shelf Sci. 49 (1999) 775–787.
[44] C.-C. Shen, H. Cheng, R.L. Edwards, S.B. Moran, H.N. Edmonds, J.A. Hoff, R.B. Thomas, Measurement of attogram quantities of ^{231}Pa in dissolved and particulate fractions of seawater by isotope dilution thermal ionization mass spectroscopy, Anal. Chem. 75 (2003) 1075–1079.
[45] C.-C. Shen, R.L. Edwards, H. Cheng, J.A. Dorale, R.B. Thomas, S.B. Moran, S.E. Weinstein, M. Hirschmann, Uranium and thorium isotopic and concentration measurements by magnetic sector inductively coupled plasma mass spectrometry, Chem. Geol. 185 (2002) 165–178.
[46] M. Stuiver, P. Reimer, J.B.E. Bard, G. Burr, K. Hughen, B. Kromer, F. McCormac, J. Plicht, M. Spurk, INTCAL98 Radiocarbon Age Calibration, 24,000-0 cal BP, Radiocarbon 40 (1998) 1041–1083.
[47] C.-H. Wang, W.C. Burnett, Holocene mean uplift rates across an active plate-collision boundary in Taiwan, Science 248 (1990) 204–206.
[48] Y.-G. Chen, T.-K. Liu, Holocene radiocarbon dates in Hengchun Peninsula and their neotectonic implications, J. Geol. Soc. China 36 (1993) 457–479.
[49] H.-T. Sun, Coral-based reconstruction of the climate for southern Taiwan during Holocene Maximum, Master Thesis,

National Taiwan Univ., Taiwan, ROC, 1998, 65 pp (in Chinese).
[50] C.-C. Shen, L.-A. Lee, C.-F. Dai, T. Lee, Improved subsampling method for biogenic skeletons and detailed growth pattern of *Porites* coral, Proc. 4th Taiwan Conference of Coral Reef Biology, 1996, pp. 246–255 (in Chinese).
[51] C.A.M. Brenninkmeijer, P.D. Morrison, An automated system for isotopic equilibration of CO_2 and H_2O for ^{18}O analysis of water, Chem. Geol. 66 (1987) 21–26.
[52] C.-C. Shen, High precision analysis of Sr/Ca ratio and its environmental application, PhD thesis, Tsing-Hua Univ., Taiwan, ROC, 1996, 187 pp.
[53] C.-C. Shen, K.-K. Liu, M.-Y. Lee, T. Lee, C.-H. Wang, H.-J. Lee, Tracing coastal water masses with Sr/Ca ratio and salinity in Nanwan Bay, Taiwan, Estuar. Coast. Shelf Sci., (in press), doi:10.1016/j.ecss.2005.05.10.
[54] T.M. Quinn, F.W. Taylor, T.J. Crowley, S.M. Link, Evaluation of sampling resolution in coral stable isotope records: a case study using records from New Caledonia and Tarawa, Paleoceanography 11 (1996) 529–542.
[55] NCOR (National Center for Ocean Research), 1985–98 CTD database from Ocean Data Bank, 2005. Available at http://www.ncor.ntu.edu.tw/ODBS/odbs_old/.
[56] R.G. Fairbanks, M.N. Evans, J.L. Rubenstone, R.A. Mortlock, K. Broad, M.D. Moore, C.D. Charles, Evaluating climate indices and their geochemical proxies measured in corals, Coral Reefs 16 (1997) S93–S100.
[57] S.J. Fallon, M.T. McCulloch, C.A. Alibert, Examining water temperature proxies in *Porites* corals from the Great Barrier Reef: a cross-shelf comparison, Coral Reefs 22 (2003) 389–404.
[58] C.-C. Shen, D.W. Hastings, T. Lee, C.-H. Chiu, M.-Y. Lee, K.-Y. Wei, R.L. Edwards, High precision glacial–interglacial benthic foraminiferal Sr/Ca records from the equatorial Atlantic Ocean, Earth Planet. Sci. Lett. 190 (2001) 197–209.
[59] H.M. Stoll, D.P. Schrag, Effects of Quaternary sea level cycles on strontium in seawater, Geochim. Cosmochim. Acta 62 (1998) 1107–1118.
[60] C.-H. Chiu, Long-term sea surface temperature records deduced from Lutao coral Sr/Ca ratios, PhD thesis, Institute of Oceanography, National Taiwan Univ., TAiwan, ROC, 1999, 162 pp. (in Chinese).
[61] C.-H. Wang, C.-J. Chang, Y.-L. Lin, W.-C. Liu, L.-A. Li, C.-S. Gieng, B.-C. Chang, W.-S. Lan, Natural recharge to the groundwaters in the Pingtung Plain, Taiwan: isotope evidences, Annual study report of National Science Council, Taiwan, ROC, 1996, 72 pp. (in Chinese).
[62] S.-C. Huang, T.-Y. Tang, Hydrographic Databank Report, Volume I, Regional Instrument Center of R/V Ocean Researcher I, National Science Council, Taipei, Taiwan, ROC, 1992.
[63] L.B. Railsback, T.F. Anderson, S.C. Ackerly, J.L. Cisne, Paleoceanographic modeling of temperature–salinity profiles from stable isotope data, Paleoceanogragraphy 4 (1989) 585–591.
[64] A.L. Berger, Long-term variations of daily insolation and Quaternary climatic changes, J. Atmos. Sci. 35 (1978) 2362–2367.
[65] J.E. Kutzbach, P.J. Guetter, The influence of changing orbital parameters and surface boundary conditions on climate simulations for the past 18,000 years, J. Atmos. Sci. 43 (1986) 1726–1759.
[66] COHMAP (Cooperative Holocene Mapping Project) Project Members, Climatic changes of the last 18,000 years: observations and model simulations, Science 24 (1988) 1043–1052.
[67] R.G. Fairbanks, A 17,000-year glacio-eustatic sea level record: influence of glacial melting rates on the Younger Dryas event and deep-ocean circulation, Nature 342 (1989) 637–642.
[68] E. Bard, B. Hamelin, R.G. Fairbanks, A. Zindler, Calibration of the ^{14}C timescale over the past 30,000 years using mass spectrometric U–Th ages from Barbados corals, Nature 345 (1990) 405–410.
[69] J. Chappell, A. Omura, T. Esat, M.T. McCulloch, J. Pandolfi, Y. Ota, B. Pillans, Reconciliation of late Quaternary sea levels derived from coral terraces at Huon Peninsula with deep sea oxygen isotope records, Earth Planet. Sci. Lett. 141 (1996) 227–236.
[70] C.-Y. Huang, P.-M. Liew, M. Zhao, T.-C. Chang, C.-M. Kuo, M.-T. Chen, C.-H. Wang, L.-F. Zheng, Deep sea and lake records of the Southeast Asian paleomonsoons for the last 25 thousands years, Earth Planet. Sci. Lett. 146 (1997) 59–72.
[71] Z. An, S.C. Porter, J.E. Kutzbach, X. Wu, S. Wang, X. Liu, X. Li, W. Zhou, Asynchronous Holocene optimum of the East Asian monsoon, Quat. Sci. Rev. 19 (2000) 743–762.
[72] J. Xiao, T. Nakamura, H. Lu, G. Zhang, Holocene climate changes over the desert/loess transition of north-central China, Earth Planet. Sci. Lett. 197 (2002) 11–18.
[73] C. Chou, Land–sea heating contrast in an idealized Asian summer monsoon, Clim. Dyn. 21 (2003) 11–25.
[74] H. Weng, K.-M. Lau, Y. Xue, Multi-scale summer rainfall variability over China and its long-term link to global sea surface temperature variability, J. Meteorol. Soc. Jpn. 77 (1999) 845–857.
[75] H.-H. Hsu, X. Liu, Relationship between the Tibetan Plateau heating and East Asian summer monsoon rainfall, Geophys. Res. Lett. 30 (2003) 2066–2069.
[76] S. Bony, J.-P. Duvel, H.L. Treut, Observed dependence of the water vapor and clear-sky greenhouse effect on sea surface temperature: comparison with climate warming experiments, Clim. Dyn. 11 (1995) 307–320.